esa

ECOSPHERE

SPECIAL FEATURE: EMPIRICAL PERSPECTIVES FROM MATHEMATICAL ECOLOGY

A new variance ratio metric to detect the timescale of compensatory dynamics

Lei Zhao[1,2,†] Shaopeng Wang[3] Lauren M. Hallett[4] Andrew L. Rypel[5] Lawrence W. Sheppard[2] Max C. N. Castorani[6] Lauren G. Shoemaker[7] Kathryn L. Cottingham[8] Katharine Suding[9] and Daniel C. Reuman[2,10]

[1]*Beijing Key Laboratory of Biodiversity and Organic Farming, College of Resources and Environmental Sciences, China Agricultural University, Beijing 100193 China*
[2]*Department of Ecology and Evolutionary Biology and Kansas Biological Survey, University of Kansas, Higuchi Hall, 2101 Constant Avenue, Lawrence, Kansas 66047 USA*
[3]*Department of Ecology, College of Urban and Environmental Science, and Key Laboratory for Earth Surface Processes of the Ministry of Education, Peking University, Beijing 100080 China*
[4]*Environmental Studies Program and Department of Biology, University of Oregon, Eugene, Oregon 97403 USA*
[5]*Department of Wildlife, Fish, & Conservation Biology, University of California Davis, Davis, California 95616 USA*
[6]*Department of Environmental Sciences, University of Virginia, Charlottesville, Virginia 22904 USA*
[7]*Botany Department, University of Wyoming, Laramie, Wyoming 82071 USA*
[8]*Department of Biological Sciences, Dartmouth College, Hanover, New Hampshire 03755 USA*
[9]*Department of Ecology & Evolution Biology, University of Colorado, Boulder, Colorado 80303 USA*
[10]*Laboratory of Populations, Rockefeller University, 1230 York Avenue, New York, New York 10065 USA*

Citation: Zhao, L., S. Wang, L. M. Hallett, A. L. Rypel, L. W. Sheppard, M. C. N. Castorani, L. G. Shoemaker, K. L. Cottingham, K. Suding, and D. C. Reuman. 2020. A new variance ratio metric to detect the timescale of compensatory dynamics. Ecosphere 11(5):e03114. 10.1002/ecs2.3114

Abstract. Understanding the mechanisms governing ecological stability—why a property such as primary productivity is stable in some communities and variable in others—has long been a focus of ecology. Compensatory dynamics, in which anti-synchronous fluctuations between populations buffer against fluctuations at the community level, are a key theoretical mechanism of stability. Classically, compensatory dynamics have been quantified using a variance ratio approach that compares the ratio between community variance and aggregate population variance, such that a lower ratio indicates compensation and a higher ratio indicates synchrony among species fluctuations. However, population dynamics may be influenced by different drivers that operate on different timescales, and evidence from aquatic systems indicates that communities can be compensatory on some timescales and synchronous on others. The variance ratio and related metrics cannot reflect this timescale specificity, yet have remained popular, especially in terrestrial systems. Here, we develop a timescale-specific variance ratio approach that formally decomposes the classical variance ratio according to the timescales of distinct contributions. The approach is implemented in a new R package, called tsvr, that accompanies this paper. We apply our approach to a long-term, multisite grassland community dataset. Our approach demonstrates that the degree of compensation vs. synchrony in community dynamics can vary by timescale. Across sites, population variability was typically greater over longer compared to shorter timescales. At some sites, minimal timescale specificity in compensatory dynamics translated this pattern of population variability into a similar pattern of greater community variability on longer compared to shorter timescales. But at other sites, differentially stronger compensatory dynamics at longer compared to shorter timescales produced lower-than-expected community variability on longer timescales. Within every site, there were plots that exhibited shifts in the strength of compensation between timescales. Our results highlight that compensatory vs. synchronous dynamics are intrinsically timescale-dependent concepts, and our timescale-specific variance ratio provides a metric to quantify timescale specificity and relate it back to the classic variance ratio.

Key words: community stability; compensatory dynamics; Special Feature: Empirical Perspectives from Mathematical Ecology; synchrony; timescale; tsvr; variance ratio.

Received 9 November 2019; revised 31 January 2020; accepted 11 February 2020. Corresponding Editor: Gabriela C. Nunez-Mir.

† E-mails: lei.zhao@cau.edu.cn

Introduction

The stability of ecosystem functions is central to the reliable provisioning of ecosystem services (Oliver et al. 2015), and understanding mechanisms underlying ecological stability is a fundamental goal of ecology (MacArthur 1955). A key insight into ecosystem dynamics is that stable aggregate functions such as total productivity can be composed of highly variable components (Gonzalez and Loreau 2009). For example, compensatory dynamics stabilize productivity when different populations have offsetting fluctuations, such that increases in the abundance or biomass of one or more species are accompanied by decreases in others (Schindler 1990, Bai et al. 2004, Hallett et al. 2014). Conversely, when species increase or decrease together (e.g., when species share responses to an external driver), the resulting synchrony increases aggregate community variability (Houlahan et al. 2007, Keitt 2008).

Population fluctuations are ubiquitous. Consequently, characterizing patterns of species fluctuations over time and in relation to each other is essential to understand stability. Importantly, population fluctuations can be shaped by a variety of drivers that operate on different timescales. For example, acute disturbances are a strong predictor of population dynamics in some systems (e.g., heavy rainfall events or cold winters regulating insect dynamics; Mutshinda et al. 2011). In other systems, population dynamics are driven by long-term climate cycles (Mantua et al. 1997, Sheppard et al. 2016). As a result, communities may exhibit a timescale specificity such that synchrony (or compensation) among species can occur at some timescales but not others (Downing et al. 2008, Keitt 2008). Moreover, the co-occurrence of short- and long-timescale drivers in the same system may result in communities that are synchronous over some timescales but compensatory over others (idealized in Fig. 1).

Evaluating timescale specificity in community variability has a tradition in aquatic ecology (Vasseur et al. 2005; 2014; Keitt and Fischer 2006; Vasseur and Gaedke 2007; Downing et al. 2008; Keitt 2008; Brown et al. 2016), but methods used there have typically relied on data-hungry techniques that may not be appropriate for shorter time series. For example, Vasseur et al. (2005) found that phytoplankton in Lake Constance showed compensatory dynamics at sub-annual timescales, driven by grazing and competition for nutrients, but synchronous dynamics at most other timescales. Downing et al. (2008) described how zooplankton in experimental ponds had synchronous dynamics at short timescales (~10 d), but had compensatory dynamics at longer timescales (~80 d). Overall, synchrony has tended to be more common than compensatory dynamics in freshwater plankton communities, and the timescales at which compensatory dynamics occur appear to be system-specific (Vasseur et al. 2014, Brown et al. 2016). Timescale-dependent approaches have facilitated a deeper understanding of community stability in freshwaters.

Compensatory dynamics have been the subject of debate in terrestrial systems. Some studies find general evidence for compensatory dynamics (Bai et al. 2004, Hector et al. 2010), others find them to be context-dependent (Grman et al. 2010, Hallett et al. 2014, Xu et al. 2015), and others conclude that synchronous dynamics dominate terrestrial systems (Houlahan et al. 2007, Valone and Barber 2008). To date, terrestrial ecologists have relied exclusively on metrics that do not incorporate timescale (most commonly, those developed by Schluter 1984, Loreau and de

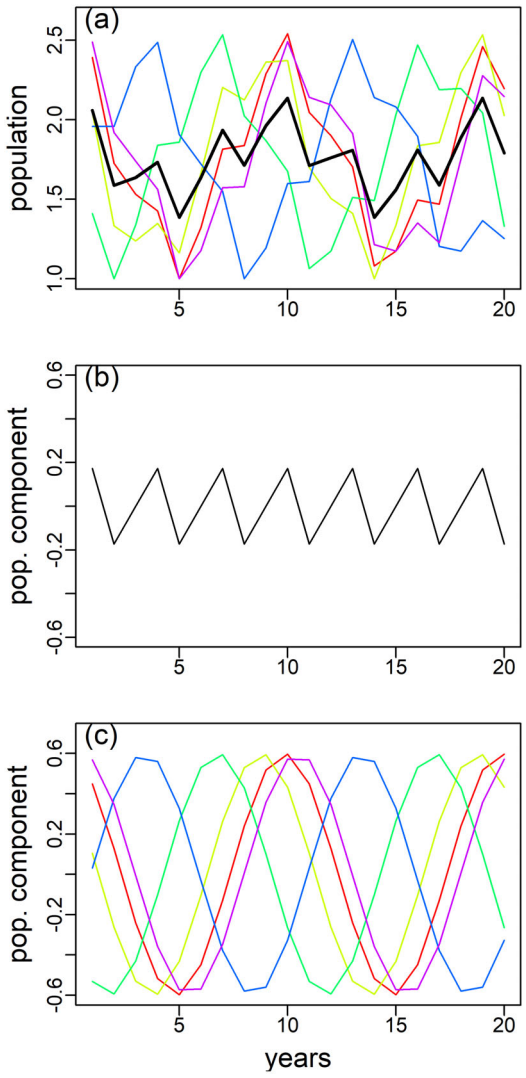

Fig. 1. Introduction to concepts using an idealized example. Five population time series (a, colors distinguish the time series; the black line is the average) were constructed by summing a sine wave of period (timescale) 3 yr and amplitude 0.2 (b) with five randomly and independently phase-shifted sine waves of period 10 yr, amplitude 0.6 (c), and then vertically shifting each time series to have minimum value 1. Thus, the time series of panel a were constructed to be synchronous on the 3-yr timescale and asynchronous (randomly related) on the 10-yr timescale. However, the classical variance ratio (Peterson 1975, Schluter 1984) was 1.06, suggesting that the species show neither compensation nor synchrony across the entire time series, missing the deliberately constructed timescale-specific processes.

Mazancourt 2008, Hallett et al. 2014). These types of analysis originated with the classic variance ratio, which can be calculated for the shorter time series available in these systems (Schluter 1984). The variance ratio compares the variance of the aggregate community to the expected variance under the assumption of independent species population fluctuations. A variance ratio greater than one indicates that populations are generally synchronous, whereas a variance ratio less than one indicates compensation (Peterson 1975, Schluter 1984). This simplicity and ease of interpretation has held wide appeal (Gotelli 2000, Houlahan et al. 2007, Winfree and Kremen 2009). However, the variance ratio cannot disentangle the timescales at which dynamics occur (Fig. 1), ultimately hindering possibilities for considering mechanisms of dynamics.

Here, we develop and apply a new timescale-specific variance ratio appropriate for terrestrial grasslands and other systems with shorter, regularly spaced time series. In contrast to timescale-specific approaches previously used on plankton data, our techniques provide a formal decomposition by timescale of the classic variance ratio approach, so that appropriately averaging/summing the components of the new approach across timescales recovers the classic non-timescale-specific results; one can then quantify the contributions of timescale bands as well as individual timescales. We first develop the theory that underlies our approach and provides timescale-specific measures of community and population variability. Second, we apply this theory to long-term (11–30 yr) records of plant community composition at six grasslands across the United States (Hallett et al. 2014). We address the fundamental questions of (1) whether synchrony/compensatory dynamics are timescale-dependent phenomena and (2) whether compensatory dynamics are rare, compared to synchrony, in grassland systems, as appears true for plankton systems (Vasseur et al. 2005; 2014; Keitt and Fischer 2006; Vasseur and Gaedke 2007; Downing et al. 2008; Keitt 2008; Brown et al. 2016). We aim to demonstrate that our timescale-specific methods can deepen understanding of grassland community dynamics (Hallett et al. 2014). Finally, we provide a software package for the R language to facilitate adoption of our techniques.

Theory

Community dynamics data are commonly abundance (e.g., count, density, percent cover, or biomass) time series $x_i(t)$ for times $t = 1,\ldots T$ for the taxa $i = 1,\ldots S$ comprising a community (e.g., all plant species in a quadrat). We denote $\mu_i = \text{mean}(x_i(t))$ and $\nu_{ij} = \text{cov}\big(x_i(t), x_j(t)\big)$ as the means and covariances, respectively, of population dynamics through time. Note that $\nu_{ii} = \text{cov}(x_i(t), x_i(t))$ is equal to the variance of $x_i(t)$. We denote $x_{\text{tot}}(t) = \sum_i x_i(t)$ as the total population density or biomass time series, and $\mu_{\text{tot}} = \sum_i \mu_i$ and $\nu_{\text{tot}} = \sum_{i,j} \nu_{ij}$ as the mean and variance, respectively, through time of $x_{\text{tot}}(t)$.

We use the square of the coefficient of variation of $x_{\text{tot}}(t)$, $\text{CV}^2_{\text{com}} = \nu_{\text{tot}}/\mu^2_{\text{tot}} = \sum_{i,j} v_{ij}/\left(\sum_i \mu_i\right)^2$, to quantify the variability of the summed community property (Wang and Loreau 2014). If populations were independent, the covariances ν_{ij} for $i \neq j$ would be 0 and CV^2_{com} would equal $\sum_i \nu_{ii}/\left(\sum_i \mu_i\right)^2 = \sum_i \nu_{ii}/\mu^2_{\text{tot}}$, which we denote as $\text{CV}^2_{\text{com\_ip}}$. We refer to $\text{CV}^2_{\text{com\_ip}}$ as the aggregate population dynamical variability of the system because it represents the degree of overall community variability that would result solely from the dynamics of individual taxa, discounting interactions.

The classic variance ratio $\varphi = \nu_{\text{tot}}/\sum_i \nu_{ii} = \sum_{i,j} \nu_{ij}/\sum_i \nu_{ii}$ (Schluter 1984) is well-known to quantify the extent to which population fluctuations of different taxa reinforce each other (through synchrony of temporal fluctuations, $\varphi > 1$) or cancel (through compensation, $\varphi < 1$) in the community total time series $x_{\text{tot}}(t)$. The variance ratio satisfies $\text{CV}^2_{\text{com}} = \varphi \text{CV}^2_{\text{com\_ip}}$ (theorem 2 of Appendix S1: Section 2; Peterson 1975, Schluter 1984). Thus, values $\varphi > 1$ (respectively, <1) correspond to greater (resp., lesser) community variability than would be expected if dynamics of different taxa were independent, reflecting synchronous (resp., compensatory) dynamics.

Next, we develop timescale-specific statistics using spectral methods, which are a standard statistical tool in ecology (Vasseur and Gaedke 2007, Defriez et al. 2016) and other fields. All definitions and computational choices about the basics of power spectra and cospectra are detailed in Appendix S1: Section 1. The power spectrum of the time series $x_i(t)$, here denoted $s_{ii}(\sigma)$ and defined for timescales of oscillation $\sigma = T/(T-1), T/(T-2), \ldots, T/2, T$, decomposes $\text{var}(x_i(t))$ by timescale in the sense that $s_{ii}(\sigma)$ will tend to be larger for timescales σ on which $x_i(t)$ is oscillating strongly. Thus, the power spectrum provides information on the dominant timescales of oscillation in $x_i(t)$. The power spectrum is a formal decomposition of variance across timescales because $\sum_\sigma s_{ii}(\sigma) = \text{var}(x_i(t))$ (Appendix S1: Section 1). The cospectrum $s_{ij}(\sigma)$ of $x_i(t)$ and $x_j(t)$ decomposes $\text{cov}\big(x_i(t), x_j(t)\big)$ by timescales, that is, $s_{ij}(\sigma)$ is defined for $\sigma = T/(T-1), T/(T-2), \ldots, T/2, T$, such that $\sum_\sigma s_{ij}(\sigma) = \text{cov}\big(x_i(t), x_j(t)\big)$ (Appendix S1: Section 1), and $s_{ij}(\sigma)$ tends to be larger for timescales on which the two time series predominately covary (i.e., they are varying synchronously, with substantial and largely in-phase periodic components at those timescales).

Community variability $\text{CV}^2_{\text{com}} = \nu_{\text{tot}}/\mu^2_{\text{tot}} = \sum_{i,j} \nu_{ij}/\mu^2_{\text{tot}}$ is made timescale-specific by replacing the covariances in the numerator with their timescale decompositions, $\text{CV}^2_{\text{com}}(\sigma) = \sum_{i,j} s_{ij}(\sigma)/\mu^2_{\text{tot}}$. Thus $\sum_\sigma \text{CV}^2_{\text{com}}(\sigma) = \text{CV}^2_{\text{com}}$ (theorem 1 in Appendix S1: Section 2), and $\text{CV}^2_{\text{com}}(\sigma)$ reveals to what extent fluctuations on each timescale contribute to community variability through time. Aggregate population variability $\text{CV}^2_{\text{com\_ip}} = \sum_i \nu_{ii}/\mu^2_{\text{tot}}$ is made timescale-specific again by replacing the variances in the numerator with their timescale decompositions, $\text{CV}^2_{\text{com\_ip}}(\sigma) = \sum_i s_{ii}(\sigma)/\mu^2_{\text{tot}}$. Thus, $\sum_\sigma \text{CV}^2_{\text{com\_ip}}(\sigma) = \text{CV}^2_{\text{com\_ip}}$ (theorem 1 in Appendix S1: Section 2) and $\text{CV}^2_{\text{com\_ip}}(\sigma)$ reveals to what extent fluctuations on each timescale contribute to aggregate population variability.

A timescale-specific variance ratio can be defined by replacing covariances in the definition of φ by their timescale-specific decompositions, $\varphi_{ts}(\sigma) = \sum_{i,j} s_{ij}(\sigma)/\sum_i s_{ii}(\sigma)$. Thus, the timescale-specific variance ratio satisfies $\text{CV}^2_{\text{com}}(\sigma) = \varphi_{\text{ts}}(\sigma)\text{CV}^2_{\text{com\_ip}}(\sigma)$. Values $\varphi_{\text{ts}}(\sigma) > 1$ correspond to synchrony at timescale σ, and values $\varphi_{\text{ts}}(\sigma) < 1$ correspond to compensatory dynamics at σ. We then define the quantity $w(\sigma) = \sum_i s_{ii}(\sigma)/\sum_i \nu_{ii}$, which represents the relative amount of variation in populations across timescales. Because of the normalization in the denominator of $w(\sigma)$, $\sum_\sigma w(\sigma) = 1$. We cannot simply sum $\varphi_{\text{ts}}(\sigma)$ across timescales to recover φ. However, $\sum_\sigma w(\sigma)\varphi_{\text{ts}}(\sigma) = \varphi$, so φ is instead a weighted average across timescales of $\varphi_{\text{ts}}(\sigma)$

(Appendix S1: Section 2). The relationships between the classic quantities CV^2_{com}, $CV^2_{com\_ip}$, and φ and their timescale-specific extensions are summarized in Fig. 2, while notation is summarized in Table 1.

Community variability, aggregate population variability, and variance ratio concepts can also be defined for any range or set, Ω, of timescales: $CV^2_{com}(\Omega) = \sum_{\sigma\in\Omega} CV^2_{com}(\sigma)$, $CV^2_{com\_ip}(\Omega) = \sum_{\sigma\in\Omega} CV^2_{com\_ip}(\sigma)$, and $\overline{\varphi_{ts}}(\Omega) = (\sum_{\sigma\in\Omega} \varphi_{ts}(\sigma)\, w(\sigma))/\sum_{\sigma\in\Omega} w(\sigma)$. It can then be shown (Appendix S1: Section 2) that

$$CV^2_{com}(\Omega) = CV^2_{com\_ip}(\Omega)\overline{\varphi_{ts}}(\Omega). \quad (1)$$

Given a threshold timescale σ_{TH}, we define $\Omega_S = \{\sigma : \sigma < \sigma_{TH}\}$ as *short timescales* and $\Omega_L = \{\sigma : \sigma \geq \sigma_{TH}\}$ as *long timescales* relative to the threshold. Equation (1) for $\Omega = \Omega_L$ and $\Omega = \Omega_S$ can then be used to compare the effects of synchrony or compensatory dynamics on population and community variability at long vs. short timescales. We note that

$$CV^2_{com} = CV^2_{com}(\Omega_L) + CV^2_{com}(\Omega_S),$$
$$CV^2_{com\_ip} = CV^2_{com\_ip}(\Omega_L) + CV^2_{com\_ip}(\Omega_S),$$
$$\varphi = \overline{\varphi_{ts}}(\Omega_L)\cdot\sum_{\sigma\geq\sigma_{TH}} w(\sigma) + \overline{\varphi_{ts}}(\Omega_S)\cdot\sum_{\sigma<\sigma_{TH}} w(\sigma).$$

To illustrate, we apply the theory to the artificial example of Fig. 1. The timescale-specific variance ratio $\varphi_{ts}(\sigma)$ was greater than one for timescale $\sigma = 3$ yr and less than one for $\sigma = 10$ yr, capturing the deliberately constructed synchronous and compensatory processes at these timescales (Fig. 3a). The non-timescale-specific variance ratio $\varphi = 1.064$, being a weighted average of $\varphi_{ts}(\sigma)$ over timescales, conflated the distinct processes and thereby

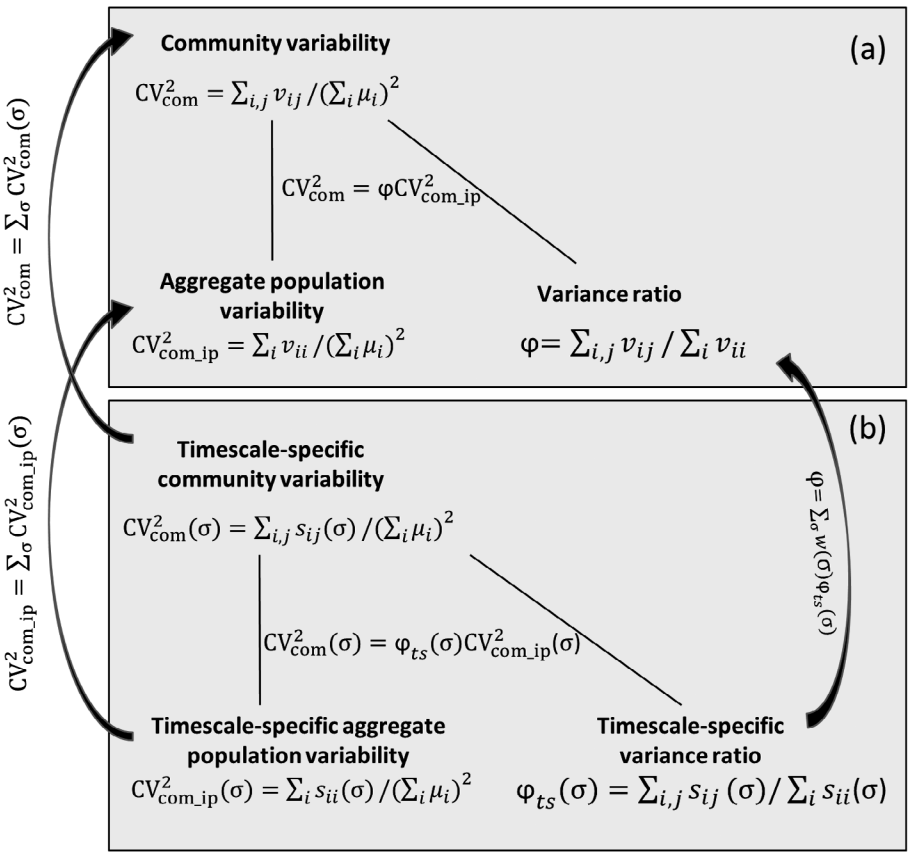

Fig. 2. Expressions of original (a) and timescale-specific (b) community variability, aggregate population variability, and the variance ratio, as well as the relationships between these quantities. A summary of notation can be found in Table 1.

Table 1. Description of symbols used in this study.

Symbol	Description
CV^2_{com}	Community variability, quantifying the variability of the summed community property
$CV^2_{com\_ip}$	Aggregate population variability, which equals the community variability when the populations are independent.
φ	Variance ratio, which is $CV^2_{com}/CV^2_{com\_ip}$
$CV^2_{com}(\sigma)$	Timescale-specific community variability on timescale σ
$CV^2_{com\_ip}(\sigma)$	Timescale-specific aggregate population variability on timescale σ
$\varphi_{ts}(\sigma)$	Timescale-specific variance ratio on timescale σ
$x_i(t)$	Time series for time t for taxon i
μ_i	Average of time series for taxon i through time, that is, mean$(x_i(t))$
ν_{ii}	Variance of time series for taxon i, that is, var$(x_i(t))$
ν_{ij}	Covariance between time series for taxa i and j, that is, cov$(x_i(t), x_j(t))$
x_{tot}	Total population density or biomass time series, that is, $\sum_i x_i(t)$
μ_{tot}	Average of the total population density or biomass time series through time
ν_{tot}	Variance of the total population density or biomass time series
$s_{ii}(\sigma)$	Power spectrum of $x_i(t)$ on timescale σ
$s_{ij}(\sigma)$	Cospectrum of $x_i(t)$ and $x_j(t)$ on timescale σ
$w(\sigma)$	Power measure, which is $\sum_i s_{ii}(\sigma)/\sum_i \nu_{ii}$

suggested neither synchronous nor compensatory dynamics. $CV^2_{com\_ip}(\sigma)$ was relatively small for $\sigma = 3$ and relatively large for $\sigma = 10$ (Fig. 3b), reflecting the use of small- and large-magnitude sinusoids, respectively, on these timescales (Fig. 1b, c). The $\sigma = 3$ oscillations had small magnitude, but were synchronous, whereas the $\sigma = 10$ oscillations had large magnitude, but were compensatory; hence, $CV^2_{com}(\sigma)$ had similar values for $\sigma = 3$ and $\sigma = 10$ (Fig. 3c). Community variability at the two timescales was due to weak synchronous oscillations for $\sigma = 3$ and strong asynchronous oscillations for $\sigma = 10$ (Fig. 3d); the distinct origins of community variability were revealed by the timescale-specific analysis but not by the classic approach.

It may at first appear as though timescale-specific results could be obtained without using Fourier methods by first performing a series of moving average operations on the data, one operation for each desired timescale, and then calculating the classic variance ratio for each moving-averaged dataset. The analysis of each moving-averaged dataset may appear to provide information on synchronous/compensatory dynamics on the timescale of averaging. However, this is incorrect, and Fourier analysis is instead the standard approach for timescale-specific analyses. The variance ratio computed on data sampled once per time interval, τ (or sampled more frequently but averaged), does not assess whether dynamics are synchronous or compensatory on the timescale τ. Rather, it assesses whether dynamics are synchronous or compensatory on average across all timescales 2τ and longer (these are the timescales that can be assessed with a sampling interval of τ). In other words, the standard variance ratio conflates all available timescales, rather than providing information solely about the timescale of sampling or averaging. Fourier analysis, invented some 200 yr ago, is the most standard approach used for the purpose of decomposing (co)variance by timescale and has been used widely for that purpose for decades.

Methods

We applied our timescale-specific variance ratio to six long-term grassland datasets from sites throughout the United States (Table S1; see Hallett et al. 2014 for detailed descriptions). Plant abundances were measured either as biomass or as percent cover. In percent-cover cases, summed values could exceed 100% due to vertically overlapping canopies. All sites were sampled annually (minimum 11 consecutive years) and were spatially replicated (at least 13 plots/site). For sites carrying out long-term experiments, we only used data from unmanipulated control plots. For all sites, methods for data collection were constant over time. One plot was omitted from the Jornada Basin Long-Term Ecological Research (LTER) site because it was an extreme outlier in community variance, leaving 47 plots from that site.

For each plot in each site, we calculated the classic variance ratio, φ; community variability, CV^2_{com}; and aggregate population variability, $CV^2_{com\_ip}$. This initial part of our analysis is a replication of work of Hallett et al. (2014). We also computed our new timescale-specific measures: the timescale-specific variance ratio, $\varphi_{ts}(\sigma)$; the power measure, $w(\sigma)$; timescale-specific community variability, $CV^2_{com}(\sigma)$;

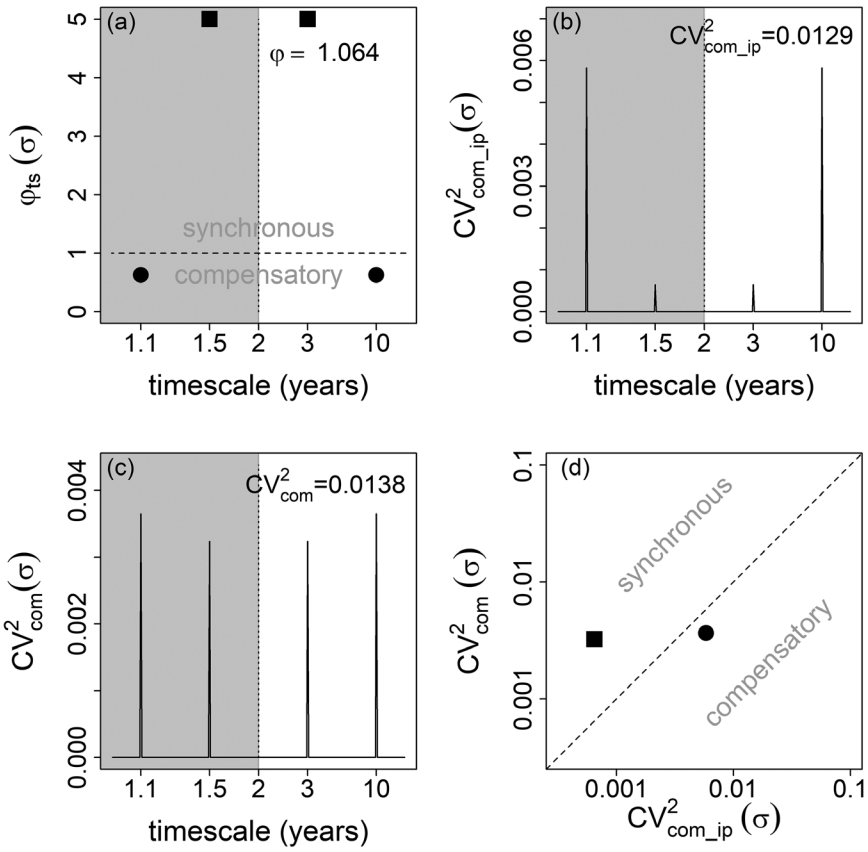

Fig. 3. Application of our theory to the artificial time series of Fig. 1. See text of the Theory section for interpretations. Panels (a–c) show the timescale-specific variance ratio $\varphi_{ts}(\sigma)$, aggregate population variability $CV^2_{com\_ip}(\sigma)$, and community variability $CV^2_{com}(\sigma)$. Timescales less than the Nyquist timescale (gray background) are symmetric to timescales greater than the Nyquist timescale (white background); we present both to reflect the underlying computation of non-timescale-specific quantities (text near top of a–c) as sums or averages across all timescales, both above and below the Nyquist timescale (Theory); but conceptually, we focus on the timescales greater than the Nyquist timescale. The horizontal dashed line (a) indicates the boundary between synchronous and compensatory dynamics for each timescale. Panel (d) compares $CV^2_{com}(\sigma)$ to $CV^2_{com\_ip}(\sigma)$ for the period-3 (square) and period-10 (circle) oscillations; the 1:1 line separates synchronous from compensatory dynamics. For simplicity, the example used sums of sinusoids, which oscillate only at discrete timescales, explaining why plotted quantities are 0 ($CV^2_{com\_ip}(\sigma)$,$CV^2_{com}(\sigma)$) or undefined ($\varphi_{ts}(\sigma)$) except at the timescales of oscillation. Real ecological signals are broadband and should typically yield plots that are well-defined and nonzero at all timescales.

timescale-specific aggregate population variability, $CV^2_{com\_ip}(\sigma)$; and the band-aggregated quantities $\overline{CV^2_{com}}(\Omega_S)$, $CV^2_{com}(\Omega_L)$, $\overline{CV^2_{com\_ip}}(\Omega_S)$, $CV^2_{com\_ip}(\Omega_L)$, $\overline{\varphi_{ts}}(\Omega_S)$, and $\overline{\varphi_{ts}}(\Omega_L)$. Sheppard et al. (2016) used the threshold σ_{TH} = 4 yr between long and short timescales because it corresponds to a frequency (1 cycle every four years) of exactly half the Nyquist frequency (the maximum rate at which periodic components of the signal can be assessed, which is 1 cycle every two years for our annual data) and because it is the boundary between persistent and anti-persistent dynamics (successive values are more similar or dissimilar, respectively) in Fourier components, measured with lag-1 autocorrelation. We use the same threshold. The Fourier quantities $s_{ij}(\sigma)$ that underlie all of our timescale-specific measures, when not averaged across timescales, are highly variable, that is, plots of these quantities against timescale are "spiky"

due to sampling variation. Averaging across timescales is the standard statistical approach for ameliorating this property (Brillinger 2001). We therefore focus our interpretations on comparisons between the long- and short-timescale bands we have defined.

To test whether short or long timescales tended to contribute more to aggregate population variability, we compared the average of $CV^2_{com\_ip}(\sigma)$ across short timescales (<4 yr) and long timescales (≥4 yr) for each plot at each site. These quantities are conceptually similar to $CV^2_{com\_ip}(\Omega_S)$ and $CV^2_{com\_ip}(\Omega_L)$, but are averages of $CV^2_{com\_ip}(\sigma)$ across short and long timescales, respectively, instead of sums. This facilitates comparisons between these quantities: Direct comparisons between $CV^2_{com\_ip}(\Omega_S)$ and $CV^2_{com\_ip}(\Omega_L)$ would be complicated by the fact that the sets Ω_S and Ω_L can have different numbers of timescales in them, in a way that depends on data time series length. Comparing the average quantities for a single plot indicated whether short or long timescales contributed more, per timescale, to aggregate population variability for that plot. Across all the plots in a site, we conducted a paired *t*-test of the significance of the difference between timescales for the site as a whole. If plots within a site can be regarded as independent replicates, *P*-value results of these tests have the usual probabilistic interpretation. If spatial autocorrelation or another factor means that plots within a site cannot be regarded as independent, then these *P*-value results should be interpreted as descriptive statistics, describing the strength of the difference between two paired distributions of values relative to the variation within the distributions. As such, we will refer to these as nominal *P*-values.

We used a similar approach to test whether short or long timescales tended to contribute more to community variability. We compared the averages of $CV^2_{com}(\sigma)$ across short and long timescales; these quantities represent the average contributions of a short or long timescale to community variability. Paired *t*-tests were again used to produce nominal *P*-values.

To test whether the degree of synchrony or compensation among populations differed by timescale, we compared $\overline{\varphi_{ts}}(\Omega_S)$ and $\overline{\varphi_{ts}}(\Omega_L)$. We again used paired *t*-tests and nominal *P*-values. These quantities reflect the extent to which either the average or the total, across the timescale band, of aggregate population variability, $CV^2_{com\_ip}(\sigma)$, explains the average or the total across the band of community variability, $CV^2_{com}(\sigma)$.

We also tested whether the averages of $CV^2_{com\_ip}(\sigma)$ across short timescales and long timescales differed significantly from each other for each plot, individually, using a randomization scheme; likewise, we tested whether the averages of $CV^2_{com}(\sigma)$ across short and long timescales differed significantly and whether $\overline{\varphi_{ts}}(\Omega_S)$ and $\overline{\varphi_{ts}}(\Omega_L)$ differed significantly, for individual plots. We explain the randomization procedure for $CV^2_{com\_ip}(\sigma)$, the other two applications being similar. Putting species abundance measures $x_i(t)$ into a matrix with rows indexed by i and columns indexed by t, we randomly permuted columns of the matrix 1000 times and computed the averages of $CV^2_{com\_ip}(\sigma)$ across short and long timescales for each randomized matrix. These randomizations will have exactly the same non-timescale-specific values $CV^2_{com\_ip}$, CV^2_{com}, and φ as the original data, but will have short- and long-timescale averages that differ from each other only due to sampling variation; so they represent a null hypothesis with no timescale structure in $CV^2_{com\_ip}$. So the difference between the short- and long-timescale averages was computed for data and compared to the distribution of values for the same statistic on randomizations. If the value of the statistic for data was greater than a fraction $1 - P/2$ or less than a fraction $P/2$ of values of the statistic for randomizations, short- and long-timescale averages of $CV^2_{com\_ip}(\sigma)$ were considered significantly different at confidence level $1 - P$.

Computations were done in R. All methods are coded into a new R package called tsvr (see *Data Availability*).

Results

Overall patterns of variability without yet accounting for timescales

Most plots exhibited compensatory dynamics when examined in aggregate across all timescales, although the strength of compensation varied across sites (Hallett et al. 2014). This provides an initial answer to question two from the *Introduction*, from a non-timescale-specific

viewpoint (but see below for a timescale-specific viewpoint): Compensatory dynamics appear to be more common in our grasslands than in plankton systems. Community variability CV^2_{com} varied widely, with a minimum observed plot-level value of 0.01 and a maximum of 1.50. Population variability $CV^2_{com\_ip}$ exhibited a similar magnitude of variability, ranging from 0.04 to 1.51. Classic variance ratios φ varied from highly compensatory to highly synchronous, that is, from 0.08 to 1.98. However, φ was less than one in 72.7% of our 150 plots. This differs significantly from 50% (nominal $P < 0.001$, two-tailed binomial test).

Timescale-specific patterns of variability

Many plots exhibited marked differences in variability and variance ratios between short and long timescales. To facilitate understanding of results, we first demonstrate this effect with data from one example plot at the Jasper Ridge Biological Preserve (JRG), before later presenting all results. Using the classic approach, dynamics at this plot would be considered compensatory: The variance ratio was 0.457 (<1), and correspondingly, CV^2_{com} (0.047) was less than $CV^2_{com\_ip}$ (0.103). However, when we decomposed variability by timescale bands, the short- and long-timescale bands showed opposite patterns (Fig. 4). The weighted average of $\varphi_{ts}(\sigma)$ across short timescales was >1, indicating synchronous dynamics, but the weighted average across long timescales was <1, indicating compensatory dynamics (Fig. 4a). Correspondingly, the average of $CV^2_{com}(\sigma)$ was slightly higher than the average of $CV^2_{com\_ip}(\sigma)$ when these averages were computed across short timescales, but was substantially less when the averages were across long timescales (Fig. 4b–d).

We applied the same approach to all 150 plots in the six sites (Fig. 5), providing a picture of how a timescale approach alters our understanding of compensatory dynamics in these systems (question one from the *Introduction*). Our data showed average (site level) greater aggregate population variability at long timescales than at short timescales at all sites (Fig. 5g–l), and likewise for community variability (Fig. 5m–r), except for the Kellogg Biological Station LTER (KBS), where the average $CV^2_{com}(\sigma)$ did not differ between short and long timescales at the site level (Fig. 4n). Thus, long timescales were the primary driver of population variability at all sites and of community variability in five of our six sites; this was not surprising given prior literature on the commonness of temporal autocorrelation in population dynamics (Halley 1996). However, the degree of synchrony and compensation among species differed substantially by timescale, at the whole-site level, at some but not all sites. Short timescales had larger weighted-average values of $\varphi_{ts}(\sigma)$ than long timescales for Jasper Ridge (JRG) and Kellogg Biological Station (KBS; Fig. 5a, b; paired *t*-test, nominal $P < 0.001$), but the weighted averages of $\varphi_{ts}(\sigma)$ over short and long timescales were not significantly different, at the site level, at the remaining four sites (Fig. 5c–f; paired *t*-test, nominal $P > 0.5$). At both JRG and KBS, the weighted-average values of $\varphi_{ts}(\sigma)$ tended to be <1 over both short and long timescales, indicating some compensation occurred across all timescales, but compensatory dynamics were stronger over long timescales.

While Jasper Ridge and Kellogg Biological Station exhibited similar timescale-specific patterns of compensatory dynamics, timescale-specific patterns of community variability differed between these sites for reasons our approach reveals. At JRG, population variability was much greater on long than on short timescales (Fig. 5g). Community variability was also higher on long timescales (Fig. 5m), but to a lesser degree than population variability, because species dynamics were more compensatory on long than on short timescales (Fig. 5a). At KBS, population variability was also higher on long than on short timescales, but less markedly so than for JRG (Fig. 5h). Because dynamics were again more compensatory on long than on short timescales for KBS (Fig. 5b), community variability was similar on short and long timescales (Fig. 5n). Thus, differences across timescales in population variability existed at both JRG and KBS, but opposing differences across timescales in the strength of compensatory dynamics were enough to eliminate timescale differences in community variability for KBS, but only to reduce them relative to population-level differences for JRG.

On average, the remaining four sites (Hayes, HAY; Jornada, JRN; Konza, KNZ; and Sevilleta, SEV) demonstrated similar strengths of compensatory dynamics across timescales

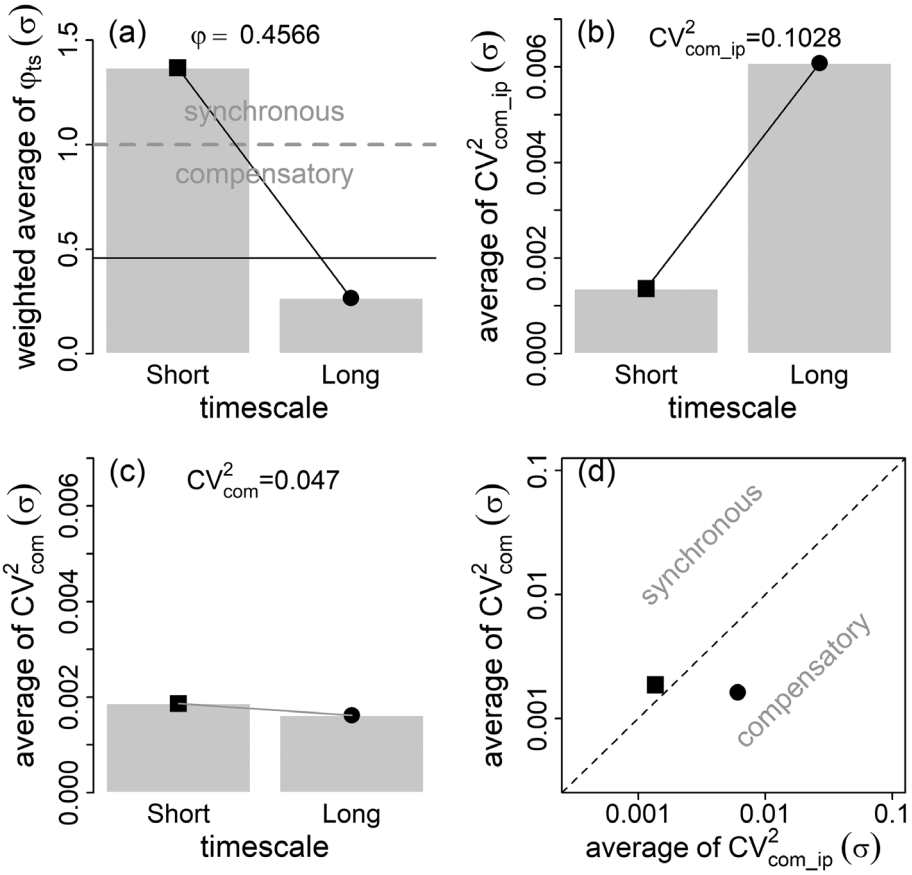

Fig. 4. Results for an example plot at the Jasper Ridge Biological Preserve (JRG), which shows a similar pattern to the artificial data of Fig. 1 (see Fig. 3). The classic, non-timescale-specific approach (text at top of a–c) suggests compensatory dynamics, and hence CV^2_{com} is less than $CV^2_{com\_ip}$. But decomposing variability by timescale bands indicated contrasting patterns at short and long timescales: The weighted average of $\varphi_{ts}(\sigma)$ was >1 across short timescales (a), so the average of $CV^2_{com}(\sigma)$ (c) was slightly greater than the average of $CV^2_{com\_ip}(\sigma)$ (b) across short timescales; whereas there reverse pattern held for long timescales. Differences between short and long timescales in panels a and b were significant, $P \approx 0$, to within the precision available from 1000 randomizations. In this figure and in Fig. 5, lines connecting timescale-specific quantities on plots will be rendered in black to indicate a significant difference ($P < 0.05$) between short and long timescales at the plot level, while gray lines indicates nonsignificant differences. Panel d compares the averages of $CV^2_{com}(\sigma)$ and $CV^2_{com\_ip}(\sigma)$ across short (square) and long (circle) timescales. See text of the *Results* section for further interpretation. The horizontal solid line in panel a shows the value of the classic variance ratio.

(Fig. 5c–f). For these sites, long timescales contributed more to both population and community variability, and to about the same extent (compare Fig. 5i, o for HAY, Fig. 5j, p for JRN, Fig. 5k, q for KNZ, and Fig. 5i, r for SEV). However, for each of these four sites there were plots that were compensatory on short timescales (short-timescale weighted average of $\varphi_{ts}(\sigma) < 1$) and synchronous on long timescales (long-timescale weighted average of $\varphi_{ts}(\sigma) > 1$), and other plots which showed the reverse pattern; and some of these differences were significant at the plot level (Fig. 5a–f, black lines). For JRG and JRN (but not for the other sites), there were substantially more significant plot-level differences between $\overline{\varphi_{ts}}(\Omega_S)$ and $\overline{\varphi_{ts}}(\Omega_L)$ than would be expected from a type I error rate.

Returning to question two from the *Introduction*, compensatory dynamics were not only more common in our grasslands than has been reported for plankton systems; for some timescales and sites, compensatory dynamics were ubiquitous: long timescales for JRG and KBS (Fig. 5a, b).

Full spectral decompositions of all quantities are in Appendix S1: Figs. S1–S6. The distributions, across plots, of all spectral quantities are given for each site in Appendix S1: Fig. S7. Comparisons between weighted-average $\varphi_{ts}(\sigma)$ and the classic variance ratio φ are made for each site in Appendix S1: Fig. S8.

Discussion

Understanding the links between diversity and stability and the mechanisms that promote them is among the long-standing goals of ecology as a field (McNaughton 1977, Tilman et al. 1998, Connell and Ghedini 2015). Although timescale specificity in population dynamics is well-established (Turchin 2003, Defriez et al. 2016, Sheppard et al. 2016), the degree to which community dynamics exhibit timescale specificity is less explored, particularly in terrestrial ecosystems. Timescale specificity in synchrony and compensatory dynamics has been demonstrated in natural and experimental freshwater plankton communities (Vasseur et al. 2005; 2014; Keitt and Fischer 2006; Vasseur and Gaedke 2007; Downing et al. 2008; Keitt 2008; Brown et al. 2016), but methods had not previously been adapted to the shorter, annually sampled time series common in terrestrial ecosystems such as grasslands. We developed and applied new methods for the timescale decomposition of the variance ratio, and of population and community variability. Our approach demonstrated the site-level value of considering timescales for two of the six sites we examined, and individual plots in other sites also appeared to show timescale structure in compensatory/synchronous dynamics. Compensatory dynamics were more common in our grasslands than has been reported for plankton systems (Vasseur et al. 2014, Brown et al. 2016), and were ubiquitous on long timescales in some sites.

In contrast to the methods which have been used to study plankton communities, our methods offer a formal decomposition of the classical variance ratio. The variance ratio and the community and population variability statistics CV^2_{com} and $CV^2_{com\_ip}$ can be recovered exactly from our timescale-specific quantities by summing or averaging appropriately over timescales. Thus, our approach formally elaborates the classical approach.

In developing our theory, we focused on the classical variance ratio (Peterson 1975, Schluter 1984). However, a distinct variance ratio of Loreau and de Mazancourt (2008), $\varphi^{(m)} = \sum_{i,j} v_{ij} / \left(\sum_i \sqrt{v_{ii}}\right)^2$, has been proposed and has become popular. This alternative approach also uses an alternative to our $CV^2_{com\_ip}(\sigma)$, which we denote $CV^2_{pop} = \left(\sum_i \sqrt{v_{ii}}\right)^2 / \left(\sum_i \mu_i\right)^2$ (Loreau and de Mazancourt 2008). We attempted a timescale-specific extension of the Loreau-de Mazancourt approach in Appendix S1: Section 3. Our derivations may facilitate future theory, but are so far not satisfactory for application to data because CV^2_{pop} does not admit a straightforward timescale decomposition.

Although some empirical evidence exists for greater community variability on long timescales (Bengtsson et al. 1997), our study appears to be the first observation of this phenomenon in grassland communities. Bengtsson et al. (1997) hypothesized that bird community variability was derived from increased population and environmental variability with time, specifically long-term trends in species abundances and temporal heterogeneity in habitat due to succession. In our study, a large proportion of population and community variability was contributed by fluctuations on long timescales (>4 yr). Yet unlike Bengtsson et al. (1997), our grassland communities were not obviously successional. Instead, a potential mechanism driving variability on long timescales in our systems may be long-term fluctuations, associated with long-timescale climatic oscillations, in the environmental resources (e.g., water and nutrients) that affect plant productivity. For example, the Pacific Decadal Oscillation (PDO) and the Atlantic Multidecadal Oscillation (AMO) contribute to long-term patterns of drought over the United States (McCabe et al. 2004), and the El Niño–Southern Oscillation (ENSO) can also be related to drought or extreme rainfall (Yoon

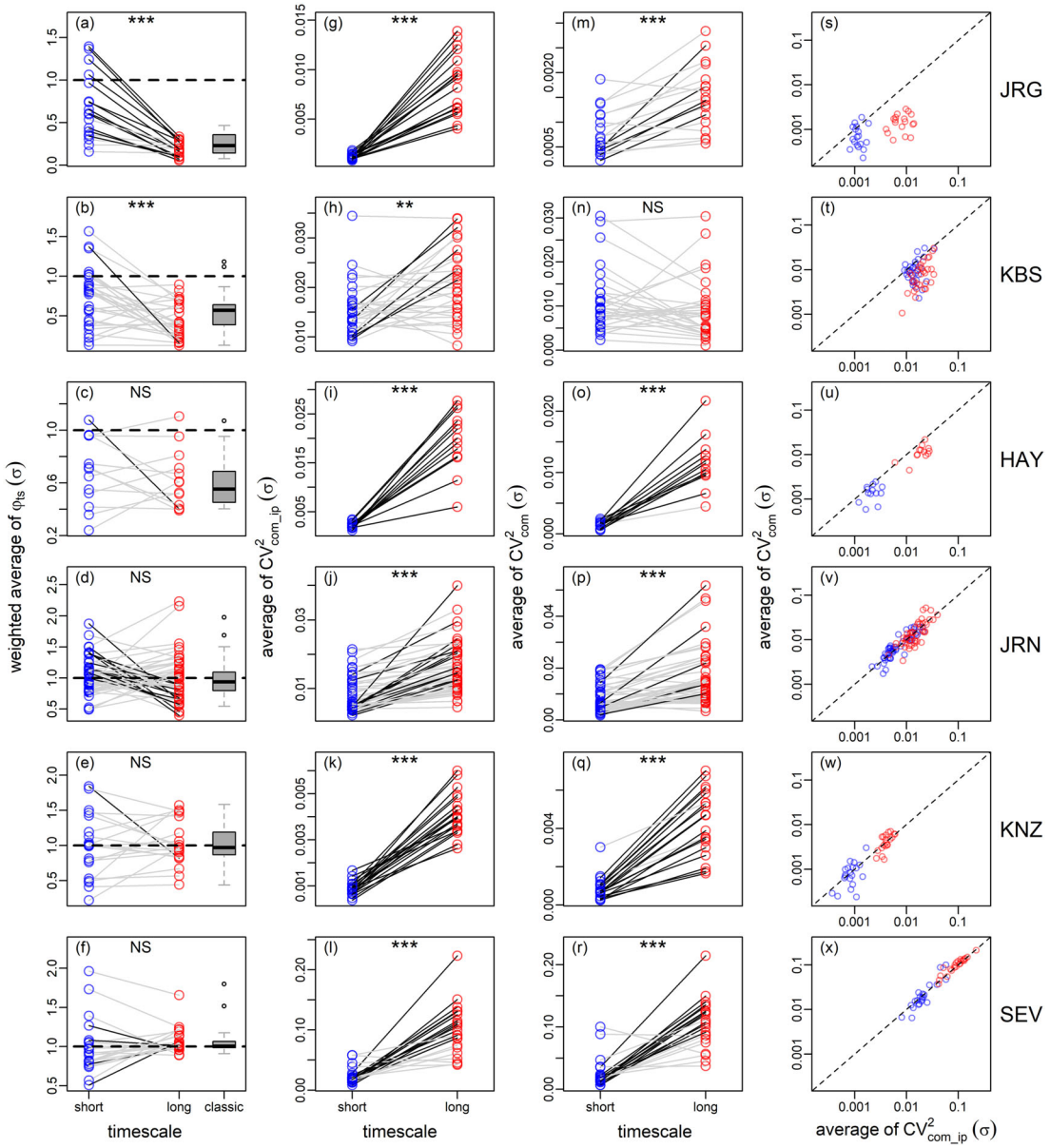

Fig. 5. Timescale-specific variance ratio, aggregate population variability, and community variability for all plots in each site. Panels parallel those in Figure 4 and show weighted averages of $\varphi_{ts}(\sigma)$ (a–f) or averages of $CV^2_{com\_ip}(\sigma)$ (g–l) or $CV^2_{com}(\sigma)$ (m–r) across short (blue) or long (red) timescales. Each pair of points on a panel is one plot. As in Fig. 4, black lines connecting timescale-specific quantities indicate a significance difference between the quantities ($P < 0.05$). Stars in each panel denote nominally significant site-level differences between short or long timescales (paired t-test): ***$P < 0.001$; **$P < 0.01$; NS: not nominally significant. The box–whisker plots in the first column of panels show distributions across plots of the classic (non-timescale-specific) variance ratio. Panels (s–x) show the relationship between the average of $CV^2_{com}(\sigma)$ and the average of $CV^2_{com\_ip}(\sigma)$ across short (blue) and long (red) timescales. Site abbreviations are JRG, Jasper Ridge Biological Preserve; KBS, Kellogg Biological Station Long-Term Ecological Research (LTER) site; HAY, Hayes, Kansas; JRN, Jornada Basin LTER; KNZ, Konza Prairie LTER; SEV, Sevilleta LTER.

et al. 2015). Long-timescale nitrogen periodicity of 8–9 yr driven by legume cycles has also been reported (Herben et al. 2017). Long-term resource variation likely propagates through ecosystems, ultimately affecting aggregate community properties in ways that depend on species interactions and shared responses to drivers. For example, plant community variability at Jasper Ridge showed a clear spectral peak at a timescale of ~10 yr. In contrast, no studies have reported greater community variability at short compared to long timescales. We speculate that community variability may generally be greater on long (>4 yr) than on shorter timescales (<4 yr).

Relatedly, our techniques have the possible limitation of not distinguishing trends from long-term oscillations in their contributions to community dynamics. This weakness should be addressed, if feasible, in future work, but the weakness is also common to prior analyses using the variance ratio and is probably an unavoidable consequence of finite-duration data. A recent study sought to separate the effects of trends and fluctuations in dynamics using detrending and a moving window approach (Lepš et al. 2019). However, aside from gathering more data, periodic fluctuations of period longer than about twice the duration of the data essentially cannot be distinguished from trends, for the simple reason that a very long-timescale periodic fluctuation can present as exactly the same pattern in a finite dataset as does a trend. The techniques of Lepš et al. (2019) effectively separate the contributions to community dynamics of both possible trends *and* very long-timescale oscillatory phenomena from the contributions due to oscillatory phenomena happening on timescales less than the duration of the data. Apparent long-term trends (which may also be long-timescale oscillations) are present even in some very long datasets (e.g., Silwood Park plant data; see Brown 1991). The argument has mathematical merit that true trends, that is, trends which continue forever, cannot occur in real ecosystems because populations and other ecological quantities cannot increase or decrease at the same rate forever. Our decision to not carry out detrending or other filtering procedures on our data prior to analysis was based on the fact that the variance ratio has traditionally been computed on non-detrended data, and our goal was to provide an extension of the method as it is commonly applied.

Decomposing community dynamics by timescale may assist in detecting the mechanisms for, and implications of, compensatory dynamics. Compensatory dynamics are promoted by at least two factors: competitive interactions and asynchronous responses to environmental change (Houlahan et al. 2007, Loreau and de Mazancourt 2013). The latter mechanism is supported by several prior studies in grasslands. For example, Hobbs et al. (2007) reported that differential responses of plant species at Jasper Ridge to a period of prolonged below-average rainfall resulted in functional compensation among species. In systems for which the consequential environmental fluctuations are connected with long-timescale environmental oscillations such as the Pacific decadal oscillation, the timescale signature of compensatory dynamics may help illuminate if the mechanism is competitive interactions or asynchronous response to environmental fluctuations.

Comparisons between our results for terrestrial grasslands and prior results with freshwater plankton suggest both similarities and differences. First, our finding of stronger compensatory dynamics at some timescales than others is broadly consistent with previous findings in plankton systems that synchrony vs. compensatory dynamics depend on timescale (Keitt and Fischer 2006, Downing et al. 2008, Vasseur et al. 2014, Brown et al. 2016). Differences by timescale were, however, less profound for grasslands than for the prior plankton studies: No grassland, at the site level, demonstrated a shift from clear compensatory dynamics on one timescale band to clear synchrony on another band, as was observed in both natural plankton populations (Vasseur et al. 2005) and experimental mesocosms (Downing et al. 2008). Finally, we did not find strong evidence of synchrony at the site level in any of our systems, unlike the general conclusion that synchronous dynamics prevailed in zooplankton in 58 lake datasets (Vasseur et al. 2014).

What level of synchrony or compensation should we expect as a norm in terrestrial vs. aquatic systems? Some have argued that we should expect overall synchronous dynamics in

communities responding to variable resources, particularly limiting resources (Loreau and de Mazancourt 2008). In contrast, others have suggested that compensatory dynamics may be the norm, especially when space is limiting or zero-sum dynamics are at play (Houlahan et al. 2007). We speculate that space limitation may shape terrestrial more than aquatic communities, which would support the occasionally strong compensatory but never strong synchronous dynamics that characterized our grassland datasets. Directional species turnover in combination with space limitation may enhance the long-term signal of compensatory dynamics in our grassland sites, as invasions often drive a decline in resident species (Pyšek et al. 2012). We expect this pattern is common to terrestrial systems, with the exception of early successional systems (Lepš et al. 2019). Finally, differences in diversity may have contributed to the more muted synchronous dynamics in terrestrial grassland than freshwater zooplankton communities. High species richness in grasslands may have buffered against strongly synchronous dynamics, as the presence of more species increases the likelihood that some will have differential responses to environmental fluctuations and thus compensatory dynamics (Ives and Hughes 2002).

Our interpretations for grasslands have focused on *average* tendencies within a particular site, either timescale specificity in the strength of compensatory dynamics (Jasper Ridge, Kellogg Biological Station) or lack thereof (Hayes, Jornada, Konza, and Sevilleta). However, variability across plots within a site was substantial, every site had some plots that were compensatory on one of the timescale bands we considered and synchronous on the other, and one site (JRN) had a large fraction of plots exhibiting significant differences between $\overline{\varphi_{ts}}(\Omega_S)$ and $\overline{\varphi_{ts}}(\Omega_L)$ (Fig. 5). When the variability we observed across plots within a site eclipses sampling variation, then timescale-specific analysis may help reveal, in future work, plot-to-plot heterogeneity in the nature and mechanisms of compensatory dynamics. Exploring potential plot-to-plot variation in the nature of community dynamics would likely have to make further use of our randomization-based method to assess the statistical significance of timescale heterogeneities in compensatory dynamics for individual plots. Studying plot-to-plot variation may provide statistical power for illuminating causes of compensatory dynamics that is lacking when making comparisons across whole sites. This can be useful future work.

Timescale dependency in the presence and magnitude of compensatory dynamics may have implications for how ecologists approach and study ecosystems more generally. For example, synthesis efforts that collate patterns of synchrony and compensation should likely consider length of time series used for such efforts or should use methods that explicitly take timescale into account. Additionally, do results drawn from short-term observations of communities following manipulation change when observed for longer periods?

To facilitate adoption of our timescale-specific approach, we developed an R package, tsvr, on CRAN. Our timescale-specific variance ratio should be particularly attractive for certain ecosystem types and applications. For example, while wavelet methods for quantifying synchrony in ecological communities are increasing in popularity and provide flexibility (Vasseur et al. 2005; 2014; Keitt and Fischer 2006; Vasseur and Gaedke 2007; Brown et al. 2016; Sheppard et al. 2016), these methods require long time series. Our methods can be used on shorter time series (e.g., >10 equally spaced time points), though we remind the reader that Fourier analysis only provides information on Nyquist timescales; inferences on timescales longer than the data are not possible. We hope our results and package will facilitate further illumination of compensatory vs. synchronous dynamics in ecological communities.

Acknowledgments

This work was part of the LTER Synchrony Synthesis Group funded by the National Science Foundation (NSF) under grant DEB#1545288, through the LTER Network Communications Office, National Center for Ecological Analysis and Synthesis (NCEAS). We thank contributors to the LTER Network, and E. Defriez, J. Dudney, S. Fey, L. Gherardi, N. Lany, M. O'Brien, C. Portales-Reyes, T. Anderson, N. Gotelli, and J. Houlahan for advice and discussions. D.C.R. and L.Z. were partly supported by the James S. McDonnell

Foundation and NSF Grants 1442595 and 1714195. L.Z. was also supported by the Beijing Natural Science Foundation (5194027) and the Chengdu Water Research Base for Ecological Civilization Construction (2018SST-02). K.L.C. was supported by the individual research and development program at NSF. L.G.S. was supported by McDonnell Foundation grant #220020513. We declare that we have no conflict of interest to this work. LZ, SW, and DCR conceived the ideas and designed the methodology while engaged in periodic discussions with all other authors; LMH provided the data; LZ, SW, LWS, and DCR analyzed the data; LZ and DCR led the writing of the manuscript, and LMH, AR, and KLC contributed substantially to writing. All authors contributed critically to the drafts and gave final approval for publication.

Literature Cited

Bai, Y., X. Han, J. Wu, Z. Chen, and L. Li. 2004. Ecosystem stability and compensatory effects in the Inner Mongolia grassland. Nature 431:181–184.

Bengtsson, J., S. R. Baillie, and J. Lawton. 1997. Community variability increases with time. Oikos 78:249–256.

Brillinger, D. R. 2001. Time series: data analysis and theory. Society for Industrial and Applied Mathematics, Philadelphia, Pennsylvania, USA.

Brown, B. L., A. L. Downing, and M. A. Leibold. 2016. Compensatory dynamics stabilize aggregate community properties in response to multiple types of perturbations. Ecology 97:2021–2033.

Brown, V. K. 1991. The effects of changes in habitat structure during succession in terrestrial communities. Pages 87–106 *in* S. S. Bell, E. D. McCoy, and H. R. Mushinsky, editors. Habitat structure: the physical arrangement of objects in space. Springer Science & Business Media, Dordrecht, The Netherlands.

Connell, S. D., and G. Ghedini. 2015. Resisting regime-shifts: the stabilising effect of compensatory processes. Trends in Ecology & Evolution 30:513–515.

Defriez, E. J., L. W. Sheppard, P. C. Reid, and D. C. Reuman. 2016. Climate change-related regime shifts have altered spatial synchrony of plankton dynamics in the North Sea. Global Change Biology 22:2069–2080.

Downing, A. L., B. L. Brown, E. M. Perrin, T. H. Keitt, and M. A. Leibold. 2008. Environmental fluctuations induce scale-dependent compensation and increase stability in plankton ecosystems. Ecology 89:3204–3214.

Gonzalez, A., and M. Loreau. 2009. The causes and consequences of compensatory dynamics in ecological communities. Annual Review of Ecology, Evolution, and Systematics 40:393–414.

Gotelli, N. J. 2000. Null model analysis of species co-occurrence patterns. Ecology 81:2606–2621.

Grman, E., J. A. Lau, D. R. Schoolmaster, and K. L. Gross. 2010. Mechanisms contributing to stability in ecosystem function depend on the environmental context. Ecology Letters 13:1400–1410.

Hallett, L. M., et al.. 2014. Biotic mechanisms of community stability shift along a precipitation gradient. Ecology 95:1693–1700.

Halley, J. M. 1996. Ecology, evolution and 1/f-noise. Trends in Ecology & Evolution 11:33–37.

Hector, A., et al. 2010. General stabilizing effects of plant diversity on grassland productivity through population asynchrony and overyielding. Ecology 91:2213–2220.

Herben, T., H. Mayerová, H. Skálová, V. Hadincová, S. Pecháčková, and F. Krahulec. 2017. Long-term time series of legume cycles in a semi-natural montane grassland: Evidence for nitrogen-driven grass dynamics? Functional Ecology 31:1430–1440.

Hobbs, R. J., S. Yates, and H. A. Mooney. 2007. Long-term data reveal complex dynamics in grassland in relation to climate and disturbance. Ecological Monographs 77:545–568.

Houlahan, J. E., D. J. Currie, K. Cottenie, G. S. Cumming, S. Ernest, C. S. Findlay, S. D. Fuhlendorf, U. Gaedke, P. Legendre, and J. J. Magnuson. 2007. Compensatory dynamics are rare in natural ecological communities. Proceedings of the National Academy of Sciences USA 104:3273–3277.

Ives, A. R., and J. B. Hughes. 2002. General relationships between species diversity and stability in competitive systems. American Naturalist 159:388–395.

Keitt, T. H. 2008. Coherent ecological dynamics induced by large-scale disturbance. Nature 454:331–334.

Keitt, T. H., and J. Fischer. 2006. Detection of scale-specific community dynamics using wavelets. Ecology 87:2895–2904.

Lepš, J., L. Götzenberger, E. Valencia, and F. de Bello. 2019. Accounting for long-term directional trends on year-to-year synchrony in species fluctuations. Ecography 42:1728–1741.

Loreau, M., and C. de Mazancourt. 2008. Species synchrony and its drivers: neutral and nonneutral community dynamics in fluctuating environments. American Naturalist 172:E48–E66.

Loreau, M., and C. de Mazancourt. 2013. Biodiversity and ecosystem stability: a synthesis of underlying mechanisms. Ecology Letters 16:106–115.

MacArthur, R. 1955. Fluctuations of animal populations and a measure of community stability. Ecology 36:533–536.

Mantua, N. J., S. R. Hare, Y. Zhang, J. M. Wallace, and R. C. Francis. 1997. A Pacific interdecadal climate oscillation with impacts on salmon production. Bulletin of the American Meteorological Society 78:1069–1080.

McCabe, G. J., M. A. Palecki, and J. L. Betancourt 2004. Pacific and Atlantic Ocean influences on multidecadal drought frequency in the United States. Proceedings of the National Academy of Sciences USA 101:4136.

McNaughton, S. J. 1977. Diversity and stability of ecological communities: a comment on the role of empiricism in ecology. American Naturalist 111:515–525.

Mutshinda, C. M., R. B. O. Hara, and I. P. Woiwod. 2011. A multispecies perspective on ecological impacts of climatic forcing. Journal of Animal Ecology 80:101–107.

Oliver, T. H., N. J. B. Isaac, T. A. August, B. A. Woodcock, D. B. Roy, and J. M. Bullock. 2015. Declining resilience of ecosystem functions under biodiversity loss. Nature Communications 6:10122.

Peterson, C. H. 1975. Stability of species and of community for the benthos of two lagoons. Ecology 56:958–965.

Pyšek, P., V. Jarošík, P. E. Hulme, J. Pergl, M. Hejda, U. Schaffner, and M. Vilà. 2012. A global assessment of invasive plant impacts on resident species, communities and ecosystems: the interaction of impact measures, invading species' traits and environment. Global Change Biology 18:1725–1737.

Schindler, D. W. 1990. Experimental perturbations of whole lakes as tests of hypotheses concerning ecosystem structure and function. Oikos 571:25–41.

Schluter, D. 1984. A variance test for detecting species associations, with some example applications. Ecology 65:998–1005.

Sheppard, L. W., J. R. Bell, R. Harrington, and D. C. Reuman. 2016. Changes in large-scale climate alter spatial synchrony of aphid pests. Nature Climate Change 6:610–613.

Tilman, D., C. L. Lehman, and C. E. Bristow. 1998. Diversity-stability relationships: Statistical inevitability or ecological consequence? American Naturalist 151:277–282.

Turchin, P. 2003. Complex population dynamics: a theoretical/empirical synthesis. Princeton University Press, Princeton, New Jersey, USA.

Valone, T. J., and N. A. Barber. 2008. An empirical evaluation of the insurance hypothesis in diversity-stability models. Ecology 89:522–531.

Vasseur, D. A., et al. 2014. Synchronous dynamics of zooplankton competitors prevail in temperate lake ecosystems. Proceedings of the Royal Society B: Biological Sciences 281:20140633.

Vasseur, D. A., and U. Gaedke. 2007. Spectral analysis unmasks synchronous and compensatory dynamics in plankton communities. Ecology 88:2058–2071.

Vasseur, D. A., U. Gaedke, K. S. McCann, and D. O. Hessen. 2005. A seasonal alternation of coherent and compensatory dynamics occurs in phytoplankton. Oikos 110:507–514.

Wang, S., and M. Loreau. 2014. Ecosystem stability in space: α, β and γ variability. Ecology Letters 17:891–901.

Winfree, R., and C. Kremen. 2009. Are ecosystem services stabilized by differences among species? A test using crop pollination. Proceedings of the Royal Society B: Biological Sciences 276:229–237.

Xu, Z., H. Ren, M. Li, J. van Ruijven, X. Han, S. Wan, H. Li, Q. Yu, Y. Jiang, and L. Jiang. 2015. Environmental changes drive the temporal stability of semi-arid natural grasslands through altering species asynchrony. Journal of Ecology 103:1308–1316.

Yoon, J., S. S. Wang, R. R. Gillies, B. Kravitz, L. Hipps, and P. J. Rasch. 2015. Increasing water cycle extremes in California and in relation to ENSO cycle under global warming. Nature Communications 6:8657.

Data Availability

Data are permanently archived at https://portal.edirepository.org/nis/mapbrowse?scope=edi&identifier=358. All methods are coded into a new R package called tsvr, available at www.github.come/reumandc/tsvr (development version) and on the Comprehensive R Archive Network (CRAN). The package includes a vignette that provides a step-by-step introduction. Codes which can reproduce the results of this study at the click of a button are at www.github.com/leiku/varrat_decomp.

Supporting Information

Additional Supporting Information may be found online at: http://onlinelibrary.wiley.com/doi/10.1002/ecs2.3114/full